AIAA JOURNAL
Vol. 33, No. 9, September 1995

Stochastic Modeling of Fracture Processes in Fiber Reinforced Composites

S. P. Yushanov*
Latvian University, Riga, Latvia
and
S. P. Joshi†
University of Texas at Arlington, Arlington, Texas 76019

The longitudinal strength of unidirectional continuous and short fiber reinforced composites is predicted by the stochastic modeling of the fracture process. The model captures the kinetics of damage evolution starting from the nucleation site to the final failure. The damage evolution is modeled by a multidimensional Markovian pure birth process. Fiber breaking, matrix cracking, and fiber/matrix interface debonding are included as interacting micromechanisms for fracture development. The probability of having a nucleation site at a particular state is calculated by the forward Kolmogorov differential equations. The transition rates of failure modes are obtained by utilizing the micromechanics based models of stress distribution. The final failure of the composite is considered to be precipitated in one of the two ways. It may be a result of a single nucleation site developing into an unstable macrocrack or may result from coalescence of arrested or stably growing damage states. The effect of the interfacial shear strength and short fiber length are studied. The analytical results show satisfactory agreement with the experimental results. Analytical predictions suggest an optimum value of the interfacial shear strength for obtaining the maximum longitudinal composite strength.

Nomenclature

b_f = interfiber spacing
C = fiber alignment factor
D = standard deviation
d_f = fiber diameter
E = Young's modulus
G = cumulative strength distribution function
g = probability density function of the strength
$K_{i,j}$ = load-transfer factor
l_d = debonding length
$\bar{l}$ = average fiber length
N = number of structural unit cells in a composite specimen
n_d = number of fiber ends with bonded interface
n_i = number of nearest intact fibers surrounding the group of i broken fibers
P = probability of composite failure
$p_{i,j}$ = probability of state $\vartheta_{i,j}$ being occupied
Q = probability of a macrocrack appearance
q_0 = probability that a randomly chosen cell contains short fiber ends
r_f = fiber radius
t_c = time to composite failure
V_f = fiber volume fraction
V_0 = composite volume
β = strength scatter parameter
δ = fiber effective length
δ_0 = gauge length
$\Theta(t)$ = two-dimensional Markovian process
$\vartheta_{i,j}$ = local damaged state with i broken fibers and j debonded interface
λ, μ = transition rate functions
σ = tensile stress
σ_f^* = local actual fiber stress
σ_0 = scale parameter for Weibull distribution of fiber tensile strength
τ_d = local fiber/matrix interfacial strength
$\tau_{\max}$ = shear stress at the fiber/matrix interface
τ_R = residual interfacial shear stress
τ_0 = scale parameter for Weibull distribution of interfacial strength distribution
ω = damage function
$\langle\rangle$ = mathematical expectation

Subscripts and Superscripts

c = composite
d = interface
e = effective stress
f = fiber
m = matrix
U = ultimate stress

Introduction

THE final composite failure is preceded by microscopic fracture nucleations and further evolution. In general, infrequent random fracture nucleates at a fraction of the final composite failure loads. Some of these fracture sites start to develop into larger damaged states predominantly due to the stress concentration in the immediate vicinity of the fracture site. In many cases, eventually one of the larger damage site evolves rapidly, forming an unstable macrocrack causing the final failure of the composite. In other cases, a large number of smaller damage sites coalesce to form the final failure path. The fracture nucleation and the subsequent evolution are significantly influenced by the local strength properties of the constituents.

The well-known probabilistic theories for the tensile strength of unidirectional composites have been proposed by Rosen[1] and Zweben[2] and further developed in detail by different authors.[3–7] These models give us a satisfactory strength estimation when the composite failure is predominantly affected by the stochastic strength distribution of reinforcement fibers but are not suitable when there are other competing fracture micromechanisms. For example, the secondary fracture processes, such as the interface

Received June 6, 1994; revision received Nov. 8, 1994; accepted for publication Nov. 22, 1994.

*Head, Laboratory of Mathematical Physics, Mathematics and Computer Science Institute; currently Visiting Scholar, Department of Mechanical and Aerospace Engineering, University of Texas at Arlington.

†Associate Professor, Department of Mechanical and Aerospace Engineering. Member AIAA.

debonding and the crack penetration into matrix, etc., may be governing fracture processes for many widely used classes of composites. The interaction between different modes of fracture micromechanisms can be investigated by the Monte Carlo simulation method.[8] But this simulation procedure requires extensive computational resources for any new set of structural parameters and properties of the composite components.

Several probabilistic theories have been proposed[9,10] to predict the strength of aligned short fiber composites. These theories are based on modification of the mixture rule,

$$\sigma_{cU} = \sigma_{fU} F + \sigma'_m (1 - V_f) \tag{1}$$

where σ_{cU} and σ_{fU} are the ultimate tensile strength of the composite and fiber, respectively, and σ'_m is the matrix stress at the ultimate tensile strain of the fiber. The probability of the clustering of short fiber ends is used for the calculation of the corrective function F. Thus, only pure "geometrical stochasticity" is taken into account in the theories based on the mixture rule. However, the problem is much more intricate due to "strength stochasticity" because of the scatter of fiber, matrix, as well as fiber/matrix interface strength properties. Both types of stochasticities for short fiber composites, the geometrical as well as the strength, can be taken into account in the approach described in this paper.

An analytical stochastic model incorporating primary and secondary fracture mechanisms and their interactions is presented. It is a kinetic type model. It allows modeling of damage evolution starting from a single fracture nucleation to the final stage of the composite failure. The following fracture micromechanisms are incorporated in the model: fiber breaks by loading and local overloading, debonding of broken fiber ends from matrix, and matrix cracks adjoining the location of fiber breaks.

The influence of interface bond strength on the composite strength and the failure morphology are investigated. Also, the influence of the fiber length and volume fraction is studied. Results are compared with the experimental observations wherever possible.

Micromechanics Modeling

A unidirectional fiber reinforced composite is considered to be made up of a very large number of unit cells which are equivalent in a stochastic sense. A cell consists of a fiber segment with bonded surrounding matrix. In the case of short fiber reinforced composite, a cell may include fiber ends. Each such cell is a probable site for the nucleation of an eventually complex fracture development. In the particular case of interest to us, the unit cell has characteristic cross-sectional dimension which is dictated by the fiber arrangement and the volume fraction, and the length dimension δ which is defined as two times the effective load-transfer length. Several definitions for the effective fiber length have been proposed. In this paper, following the classical Zweben[2] paper, Friedman's definition[11] for δ is used,

$$\delta = d_f \left(\frac{3E_f}{2E_m} \frac{1 - \sqrt{V_f}}{\sqrt{V_f}} \right)^{\frac{1}{2}} \tag{2}$$

where E_f is the fiber Young's modulus and E_m is the matrix Young's modulus.

Let $f(l)$ be the probability density function of the fiber length. Therefore, the average length is calculated by

$$\bar{l} = \left(\int_0^\infty l f(l)\, \mathrm{d}l \right) \Big/ \left(\int_0^\infty f(l)\, \mathrm{d}l \right)$$

It is obvious that

$$\int_0^\infty f(l)\, \mathrm{d}l = 1$$

It follows from considering the equilibrium of external and internal stresses that the composite stress σ_c is given by

$$\sigma_c = C \sigma_f V_f (1 - (\delta / 2\bar{l})) + \sigma_m (1 - V_f) \tag{3}$$

where σ_f and σ_m are mean fiber and matrix tensile stresses, the term $[1 - (\delta/2l)]$ accounts for the effects of stress builtup from the fiber ends, and C is a fiber alignment factor[12,13] which is equal to one for the perfect fiber alignment. In the following analysis, it is supposed that the mean fiber length far exceeds the load transfer length. By assuming strain compatibility in the composite, one can arrive at the following expression for mean tensile stress in the matrix:

$$\sigma_m = \frac{E_m}{E_f} \sigma_f \tag{4}$$

The maximum shear stress at the interface between the fiber and matrix is given by[8]

$$\tau_{\max} = \xi \sigma_f; \qquad \xi = \sqrt{\frac{E_m}{6E_f} \frac{r_f}{b_f}} \tag{5}$$

Here, b is the spacing between the adjacent fibers. If shear stress $\tau_{\max}$ at the fiber/matrix interface near the fiber end exceeds the ultimate value τ_d then the matrix debonding will develop.

Near the broken or short fiber end, the local matrix stress state is the superposition of tensile and shear stresses. It is convenient to define an equivalent or effective matrix stress as[14]

$$\sigma_{me} = \sqrt{3 J_2} \tag{6}$$

where J_2 is the second invariant of the stress deviator tensor. Combining Eqs. (4–6), one obtains the following expression for the maximum matrix effective stress:

$$\sigma_{me} = \sqrt{\sigma_m^2 + 3\tau_{\max}^2} = \eta \sigma_f; \qquad \eta = \sqrt{\left(\frac{E_m}{E_f} \right)^2 + \frac{r_f}{2b_f} \frac{E_m}{E_f}} \tag{7}$$

The matrix effective stress will be used in a local matrix failure criterion (von Mises criterion); if σ_{me} exceeds the prescribed ultimate value σ_{mU} then local matrix cracking occurs.

The intact fibers surrounding a broken fiber or a group of broken fibers are under local overloading conditions. The load-transfer factor (after Zweben[2]) $K_{i,j}$ is used to characterize these overloading conditions (i is the number of broken adjacent fibers of which j have a debonded fiber/matrix interface). For no debonding, the classical results based on the shear-lag analysis obtained by Hedgepeth[15] and Hedgepeth and Van Dyke[16] can be used for the load-transfer factor $K_{i,0}$ calculation. For debonded matrix, the problem of calculating the load-transfer factor $K_{i,j} (j \neq 0)$ is much more complex. It follows from the numerical analysis of the stress redistribution around the broken fiber with debonded matrix[8] that the overstressing of the nearest intact fibers surrounding the broken fiber with debonded interface is inversely proportional to the debonding length l_d.

$$K_{1,1} = 1 + \frac{K_{1,0} - 1}{(1 + (2l_d/\delta))} \tag{8}$$

Utilizing this result for approximating the load-transfer factor for the multiple fiber breaks with debonding yields

$$K_{i,j} = 1 + \frac{K_{i,0} - 1}{[1 + (j/i)(2l_d/\delta)]} \tag{9}$$

Several approaches have been proposed for the debonding length calculation.[17–20] Here, the approximation proposed in Ref. 8 is adopted for the debonding length evaluation. This approximation is based on the results of numerical simulation of the dynamic debonding process development and is given by the formula[8]

$$\frac{l_d}{d_f} = \frac{\sigma_f^\infty - \sigma_{f\tau}}{4\tau_R}; \qquad \sigma_f^\infty \geq \sigma_{f\tau} \tag{10}$$

where σ_f^∞ is the fiber stress far away from the fiber end, $\sigma_{f\tau}$ is the critical fiber stress level above which the fiber break will lead to the matrix debonding, and τ_R is the residual interfacial shear stress. Using Eq. (10) when $\sigma_{f\tau} = \tau_d / \xi$ and $\sigma_f^\infty = \sigma_c V_f$ one obtains the following expression for the debonding length:

$$\frac{l_d}{d_f} = \frac{\xi \sigma_c V_f - \tau_d}{4\xi \tau_R} H(\xi \sigma_c V_f - \tau_d) \tag{11}$$

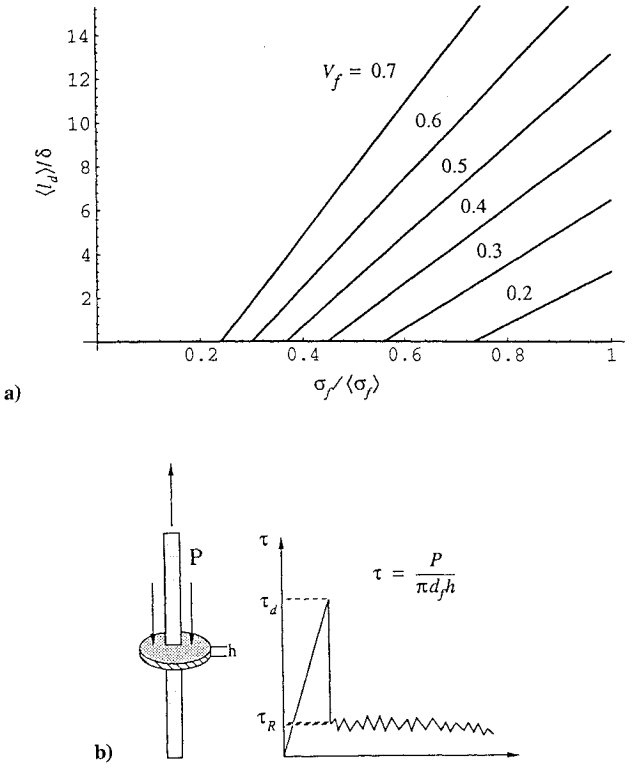

Fig. 1 a) Mean value of the matrix debonding length for carbon/epoxy composite, $\langle \tau_d \rangle / \langle \sigma_f \rangle = 0.02$, and $\tau_R = 0.1 \langle \tau_d \rangle$; and b) typical experimental measurement of the slipping frictional force τ_R at fiber/matrix interface.[21]

where $H()$ is the Heaviside unit step function. It can be seen from Eq. (11) that the debonding length depends on the composite stress level at which the fiber breaks. The interfacial shear strength τ_d has the cumulative distribution function $G_d(\tau_d)$ which is supposed to be known. It means that debonding length is also a random variable with the mean value $\langle l_d \rangle$ that is calculated from relation (11) for any known interfacial strength distribution. The typical dependence of the mean debonding length on the fiber stress for a carbon/epoxy composite (this type of the composite is adopted in the next section for numerical calculations) is shown in Fig. 1.

It can be seen from this figure that the debonding length depends on the fiber stress level at which the fiber breaks. Also, the higher is the fiber volume fraction, the longer is the debonding length. The value of the debonding length is also a function of the sliding friction force τ_R which should be determined experimentally[21,22] (see Fig. 1b).

Fracture Process Modeling

Fracture Nucleation

There are two possible modes of fracture nucleation: matrix cracking at the short fiber ends and the fiber breakdowns. These fracture nucleation modes are regulated by different micromechanisms. The first one is controlled by the local stress concentration in the matrix surrounding the fiber end and by the local matrix strength. The second one is regulated by the axial tensile stress in a fiber and its tensile strength distribution.

The fiber breakdowns and matrix cracking are random events which are specified by their respective strength distribution functions. At any moment of time t during the loading each cell may be in one and only one of the two mutually exclusive states: the cell may sojourn in an undamaged state or it may be damaged. The probability $p_{0,0}(t)$ of the cell to be in an undamaged state is

$$p_{0,0}(t) = p_0^{(f)}(t) + p_0^{(m)}(t) \tag{12}$$

where $p_0^{(f)}$ and $p_0^{(m)}$ are the probabilities of sojourning in an undamaged state for the cell without a fiber end and for the cell containing a fiber end, respectively. The transitions from undamaged state to damaged states can be considered to be the Poisson processes which are derived by differential equations

$$\dot{p}_0^{(f)}(t) = -\lambda_f(t) p_0^{(f)}(t); \qquad \dot{p}_0^{(m)}(t) = -\lambda_m(t) p_0^{(m)}(t) \tag{13}$$

under the initial conditions

$$p_0^{(f)}(0) = 1 - q_0; \qquad p_0^{(m)}(0) = q_0 \tag{14}$$

where q_0 is the probability that a randomly chosen cell contains the fiber end. This probability can be estimated as the ratio of the effective fiber length to the mean fiber length

$$q_0 = \delta / \bar{l} \tag{15}$$

In Eqs. (13) λ_f is the transition rate of fiber breakdowns, and λ_m is the transition rate of matrix cracking near the fiber end. It should be noted that the interface debonding at the end of a short fiber is not considered as a damage nucleation event because it is considered as a damage evolution event. The probability of encountering the short fiber end is incorporated as an initial condition. One can think of short fiber ends as the existing "predamaged" state. A cell containing fiber end is "actually damaged" when the attached matrix is cracked.

Transition Rates

A transition rate is determined as the density of conventional probability of the failure occurring at time t, on the condition that it has not taken place prior to this instant,

$$\lambda(t) = \lim_{\Delta t \to 0} \frac{Pr\{t \le t \le t + \Delta t \mid t > t\}}{\Delta t} \tag{16}$$

where $Pr\{A \mid B\}$ is the notation for a conventional probability. This probability may be expressed by means of the distribution function $G(t \le t)$ of the time to start of the failure by the considered mode. Using the equation for conventional probability and carrying out the limit in Eq. (16), one obtains

$$\lambda(t) = \frac{1}{1 - G(t)} \frac{\mathrm{d}G(t)}{\mathrm{d}t} \tag{17}$$

Using Eq. (17) one obtains the following expressions for rates of fiber breakdowns and matrix cracking:

$$\lambda_f(t) = \frac{g_f(\sigma_f)}{1 - G_f(\sigma_f)} \dot{\sigma}_f; \qquad \lambda_m(t) = \frac{g_m(\sigma_{me})}{1 - G_m(\sigma_{me})} \dot{\sigma}_{me} \tag{18}$$

where g_f and g_m are the fiber breakdowns and matrix cracking differential probability distribution functions, respectively, and $\dot{\sigma}_f$ is the rate of fiber loading.

The expressions (18) for transition rates are valid when the number of damaged elements immediately before the final composite failure is quite small. In general, however, there could be cases where the increase in average stresses in cells caused by the damage accumulation cannot be neglected. To incorporate this condition, assume that the transition rates are determined by the actual averaged stresses in a cell. In particular, the actual averaged stress in a cell is approximated by averaging the stresses at an appropriate local level. It should be noted that the accuracy of the actual stress calculation depends on simplifying assumptions. According to the adopted assumption, the transition rates are calculated by using the actual stresses $\sigma^* = \sigma/(1 - \omega)$, Therefore, Eqs. (18) have to be rewritten as

$$\lambda_f(t) = \frac{g_f(\sigma_f^*)}{1 - G_f(\sigma_f^*)} \dot{\sigma}_f^*; \qquad \lambda_m(t) = \frac{g_m(\eta\sigma_f^*)}{1 - G_m(\eta\sigma_f^*)} \eta\dot{\sigma}_f^*$$

$$\sigma_f^*(t) = \sigma_f/(1 - \omega) \tag{19}$$

where σ_f is the average fiber stress whereas σ_f^* is the local actual fiber stress and ω is the damage function. Most often, ω is identified with the density of microcracks in the vicinity of the examined point or with the relative quantity of broken structural elements. Also, ω can be interpreted as the relative damaged area of the specimen.

Anyway, during the loading process the value ω should change within the limits $0 \leq \omega \leq 1$, and the value $\omega = 0$ corresponds to an undamaged material. The damage function ω will be specified later. It should be noted that this function is not known a priori and it is calculated along with the fracture process simulation.

Fracture Evolution

After nucleation, the fracture process can develop by different failure modes. At least three fracture modes are involved in this process: matrix cracking between broken and intact fibers in the gap between short fibers, fracture of the nearest fibers adjacent to the damaged zone, and matrix debonding from the broken fiber end (see Fig. 2). The realization of the specific failure mode depends on the elastic properties of the constituents as well as on fiber, matrix, and fiber/matrix interface strengths mean values and its scatters. Thus, it is not possible to predict the failure modes sequences in advance, and we can only evaluate the probabilities of all possible specific fracture paths realizations.

We define a random process $\Theta(t) = \{\vartheta_{i,j}(t); i, j = 0, 1, \ldots\}$ which allows an arbitrary volume of the composite around a fracture nucleation cell to assume discrete states $\vartheta_{i,j} (i \geq j)$ at an instant of a continuous loading process. This process is continuous in time and discontinuous in the configuration space (Fig. 3). The index i represents the number of unit fracture steps in the transverse direction. It starts from any fractured cell. Each such step represents a fiber failure and matrix cracking, not necessarily in any particular order. The index j represents the number of fracture steps in the longitudinal direction due to matrix debonding from the broken fiber end or from a short fiber end. The length of a unit fracture in this direction is governed by the fiber/matrix interface debonding length l_d. If the interface bonding strength is high enough, the fracture process develops without the interface debonding. This case corresponds to path O–A in the configuration space (Fig. 3). Another special path, O–B, corresponds to a very low debonding strength when each fiber break is accompanied be the matrix debonding from the fiber end. Thus, if a local volume is in state $\vartheta_{i,j}$, it means that the damaged volume around fracture nucleus consists of i adjacent broken fibers with the cracked surrounding matrix and j of i broken fibers with debonded interface near the broken ends. The state $\vartheta_{0,0}$ corresponds to the intact cell.

The process $\Theta(t)$ is considered an ordinary process, i.e., the probability of transition from $\vartheta_{i,j}$ to any other states are of the order of the square of the time increment, except the subsequent states $\vartheta_{i+1,j}$ or $\vartheta_{i,j+1}$ and the same state. This means that if at time t the process is in a state $\vartheta_{i,j}$ then during the subsequent time interval $[t, t + \Delta t]$ one and only one of three possible transition modes can take place: a step in the transverse direction $\vartheta_{i,j} \to \vartheta_{i+1,j}$, a step in the longitudinal direction $\vartheta_{i,j} \to \vartheta_{i,j+1}$, or the local volume can sojourn at the same state $\vartheta_{i,j}$. These conditions define a two-dimensional Markovian pure birth stochastic process, and the probabilities $p_{i,j}(t)$ to be at state $\vartheta_{i,j}$ are derived by forward Kolmogorov differential equations[23]

$$\dot{p}_{i,j}(t) = \lambda_{i-1\to i,j}(t)p_{i-1,j}(t) + \mu_{i,j-1\to j}(t)p_{i,j-1}(t) - [\lambda_{i\to i+1,j}(t) + \mu_{i,j\to j+1}(t)]p_{i,j}(t) \tag{20}$$

under the initial conditions $p_{i,j}(0) = 0$ for $i \geq 1$, $j \geq i \geq 0$, and $\mu_{i,-1\to 0} \equiv 0$. The probability $p_{0,0}(t)$ is defined by Eqs. (12–14). The transition rates in the transverse $\lambda(t)$ and in the longitudinal $\mu(t)$ directions are defined as

$$\lambda_{i\to i+1,j}(t) = \lim_{\Delta t\to 0} \frac{Pr\{\theta(t + \Delta t) = \vartheta_{i+1,j} \mid \theta(t) = \vartheta_{i,j}\}}{\Delta t} \tag{21}$$

$$\mu_{i,j\to j+1}(t) = \lim_{\Delta t\to 0} \frac{Pr\{\theta(t + \Delta t) = \vartheta_{i,j+1} \mid \theta(t) = \vartheta_{i,j}\}}{\Delta t} \tag{22}$$

Equations (20) give us the complete stochastic description of the damage evolution from each fracture nucleus. All of the information about specific fracture mechanisms of damage evolution is included in the transition rate functions.

The probability of a fracture development in the longitudinal direction is controlled by the fiber/matrix interface strength: if shear stress at the interface near the fiber end exceeds the ultimate value τ_d, then the matrix debonding occurs and the probability of this event is equal to

$$P_d = Pr\{\tau_{\max} \geq \tau_d\} = G_d(\xi\sigma_f^*)$$

where G_d is the fiber/matrix interface shear strength cumulative distribution function and the coefficient ξ is defined by Eq. (5). The rate of transition in the longitudinal direction is equal to the rate of interface debonding due to the actual stresses on the fiber/matrix interface multiplied by the number $n_d = (i - j)$ of fiber ends with bonded interface

$$\mu_{i,j\to j+1}(t) = n_d \frac{g_d(\xi\sigma_f^*)}{1 - G_d(\xi\sigma_f^*)} \xi\dot{\sigma}_f^* \tag{23}$$

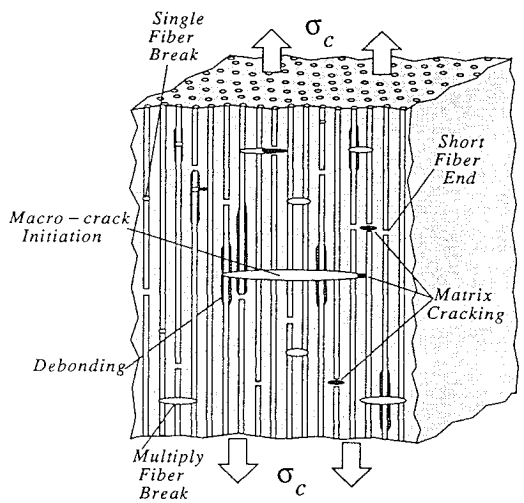

Fig. 2 Schematic of a damage development in a composite.

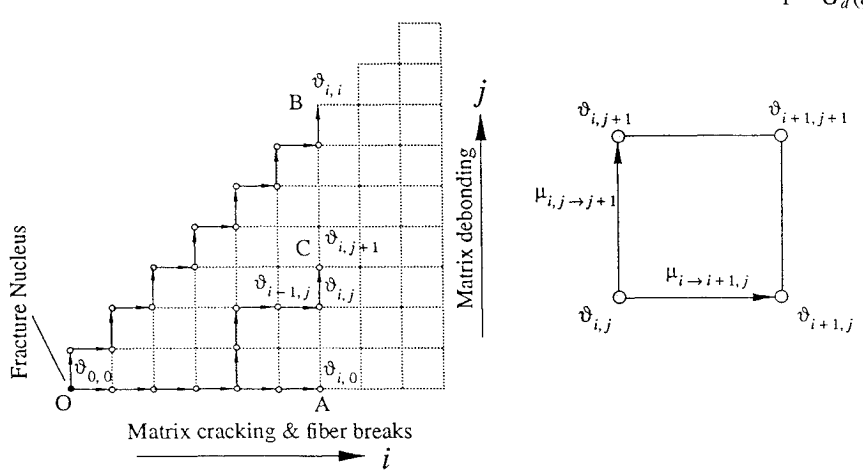

Fig. 3 Fracture process development in a configuration space.

Now, consider the rate of transition in the transverse direction. There are two distinct modes of fracture propagation in the transverse direction. First, if the short fiber end is located ahead of the crack, then a unit step in the transverse direction is only due to the matrix failure. The probability of matrix cracking when the short fiber end is encountered is equal to

$$P_1 = q_0 G_m(\sigma_{me}) \tag{24}$$

where q_0 is the probability of encountering a short fiber end just ahead of propagating crack tip. This probability is defined by formula (15). If there is no short fiber end ahead of the crack, then the adjacent matrix and fiber should fail in a unit step in the transverse direction. The probability of this event is

$$\begin{aligned} P_2 = (1-q_0)\{&G_m(\sigma_{me})[G_f(K'_{ij}\sigma_f) - G_f(K_{ij}\sigma_f)] \\ &+ G_f(K_{ij}\sigma_f)[G_m((K''_{ij})\sigma_{me}) - G_m(\sigma_{me})] \\ &+ G_m(\sigma_{me})G_f(K_{ij}\sigma_f)\} \end{aligned} \tag{25}$$

In this equation, the first term in braces is the probability of matrix cracking and immediate intact fiber failure, the second term represents the probability of fiber failure and immediate matrix cracking, and the third term is the probability of simultaneous matrix and fiber failure. Here K_{ij} is the stress concentration in the nearest intact fiber, K'_{ij} is the fiber stress concentration when the matrix is failed, and K''_{ij} is the stress concentration in the matrix located between the broken fibers.

The probabilities P_1 and P_2 correspond to mutually exclusive events and, therefore, the probability of a unit step in transverse direction is equal to the sum of these two probabilities and its rate is equal to

$$\lambda_T(t) = \frac{1}{1-P_T}\frac{dP_T}{dt}; \qquad P_T = P_1 + P_2 \tag{26}$$

A detailed micromechanical analysis should be carried out to calculate fiber and matrix stresses for each of the aforementioned failure modes. As a first approximation, we shall use the following assumption for stress concentration factors $K_{ij} = K'_{ij}$ and $K''_{ij} = 1$. With this assumption and taking into account that the failure rates are function of true stresses, multiplying Eq. (26) by the number n_i, which is the number of intact fibers surrounding the local damage state with i adjacent broken fibers, the following expression for the transition rate in the transverse direction can be obtained from Eqs. (24–26):

$$\lambda_{i\to i+1,j}(t) = n_i \frac{g_m(\eta\sigma_f^*)\eta[q_0 + (1-q_0)G_f(K_{ij}\sigma_f^*)] + (1-q_0)G_m(\eta\sigma_f^*) + g_f(K_{ij}\sigma_f^*)K_{ij}}{1 - G_m(\eta\sigma_f^*)[q_0 + (1-q_0)G_f(K_{ij}\sigma_f^*)]}\dot{\sigma}_f^* \tag{27}$$

Final Failure and Damage Function

One of the possible types of final failures of the composite is due to a single nucleating site evolving into an unstable macrocrack while the overall damage stays low. Low overall damage signifies that there is no interaction between distributed damage states. This failure mode is the result of the local stress concentration in fibers neighboring the broken ones. The criterion for this type of fracture is obtained as follows.

By definition, $p_{i,j}(t)$ are the probabilities, and the following normalizing condition is valid at any moment of time

$$\sum_{i,j=0}^{\infty} p_{i,j}(t) = 1 \tag{28}$$

Therefore, the probability $Q_i(t)$ that there will be at least i adjacent broken fibers is

$$Q_i(t) = 1 - \sum_{j=0}^{i} p_{i,j}(t) \tag{29}$$

The probability of a macrocrack formation from any fracture nucleus is defined as

$$Q(t) = \lim_{i\to\infty} Q_i(t) \tag{30}$$

In a composite with volume V_0 the maximum possible number of fracture nucleus is

$$N = 4V_0V_f/\pi d_f^2\delta \tag{31}$$

and according to Poisson distribution, the probability of a macrocrack appearance in a composite is

$$P(t) = 1 - \exp[-NQ(t)] \tag{32}$$

This is the probability distribution function for time to composite failure due to an unstable macrocrack formation. The mathematical expectation $\langle t_c\rangle$ and variance $D_{t_c}^2$ for the time to composite failure are calculated from Eq. (32) as

$$\langle t_c\rangle = \int_0^\infty tP(t)\,dt = N\int_0^\infty t\dot{Q}(t)e^{-NQ(t)}\,dt \tag{33}$$

$$D_{t_c}^2 = N\int_0^\infty t^2\dot{Q}(t)e^{-NQ(t)}\,dt - \langle t_c\rangle^2 \tag{34}$$

The mathematical expectation of the composite strength $\langle\sigma_c\rangle$ and its standard deviation D_{σ_c} are equal then

$$\langle\sigma_c\rangle = \langle t_c\rangle\dot{\sigma}_c; \qquad D_{\sigma_c} = D_{t_c}\dot{\sigma}_c \tag{35}$$

where $\dot{\sigma}_c$ is rate of loading of the composite.

The existence of a nonzero limit in Eq. (30) is possible because as i increases the rate of transition from the state with i broken fibers to the state with $(i+1)$ broken fibers also increases due to the stress concentration. In some cases, the probability of an isolated macrocrack formation is equal to zero if the stress concentration does not increase rapidly enough. In these cases the final failure is the result of coalescence of a large number of microcracks, and analysis to obtain detailed stresses distribution requires taking into account the crack interaction. However, in many realistic cases an unstable isolated macrocrack formation takes place at a low crack density before the final failure. This failure criterion is limited to such cases.

Another possible final failure criterion, as mentioned earlier, is due to the coalescence of large number of microcracks. When the damage is widespread, the final failure occurs catastrophically because distributed fractures join together forming a breaking path. A criterion for this type of final failure is defined as follows.

A measure of damage accumulation in a composite is described by the damage function $\omega(t)$ which is the relative fraction of the fractured unit cells

$$\omega(t) = \sum_{i=1}^{\infty}\left[p_{i,0}(t) + \sum_{j=1}^{i}\frac{2l_d-\delta}{\delta}H\left(l_d - \frac{\delta}{2}\right)p_{i,j}(t)\right] \tag{36}$$

The function $\omega(t)$ is not known a priori and is evaluated along with Eq. (20). The first term in Eq. (36) represents the relative fraction of broken unit cells due to fiber breakdowns. The second term is the relative numbers of unit cells which are adjacent to the cells with fiber breakdowns containing interface debonding that extended beyond the cell containing fiber breakdown. The upper bound $\omega = 1$ corresponds to breaking of all microstructure elements. A more realistic estimate can be obtained by assuming that the loss of integrity occurs if ω reaches some critical level ω^* above which dispersed damage forms a continuous fracture path. The final failure criteria is formulated then as

$$\omega(t) = \omega^* \tag{37}$$

Table 1 Properties of fiber, matrix, interface, and composite tensile strengths[26,27]

Material	Tensile modulus, MPa	Tensile strength, MPa	Interfacial shear strength, MPa	Composite tensile strength, $V_f \approx 0.677$, MPa
AU-4	234	3585	37.2	1403 ± 107
AS-4	234	3585	68.3	1890 ± 143
AS-4C	234	3585	81.4	2044 ± 256
EPON 828	3.6	89.6	—	—

For any finite lattice, percolation thresholds are random, and their distributions are narrower for larger lattices. These distributions are roughly Gaussian. As has been shown in Ref. 24, the percolation threshold decreases with increasing inhomogeneity. The percolation threshold varies between the limits 0.5 and 0.59. A value of $\omega^* \approx 0.59$ is used in this paper. It is based on the two-dimensional site percolation threshold.

Numerical Simulation

Input Data

The Weibull distribution function $G_f(\sigma_f)$ is used to describe the strength of fibers. This distribution is written in the form

$$G_f(\sigma_f) = 1 - \exp\left[-\frac{\delta}{\delta_0}\left(\frac{\sigma_f}{\sigma_0}\right)^{\beta_f}\right] \tag{38}$$

where σ_0 and β_f are the parameters of the Weibull distribution, δ is the effective length, δ_0 is the length dimension utilized in obtaining the distribution parameters, and σ_f is the nominal fiber stress. The mean strength of a fiber of length δ is computed to be, from Eq. (38),

$$\langle \sigma_f \rangle = \sigma_0(\delta_0/\delta)^{1/\beta_f}\Gamma(1 + 1/\beta_f)$$

where $\Gamma(\,)$ is the gamma function.

The distribution of the interfacial shear strength depends on the statistical nature of the properties of matrix and interface, which should be determined experimentally.[25] The distribution function of the interfacial strength τ_d is also assumed to be the Weibull distribution with parameters τ_0 and β_d which are the scale and shape parameters, correspondingly. The cumulative distribution function of the local matrix strength, σ_{mU} is also approximated by the Weibull distribution with parameters σ_{m0} and β_m. These distributions are written in the form:

$$\begin{aligned} G_d(\tau_d) &= 1 - \exp(-\tau_d/\tau_0)^{\beta_d}; \\ G_m(\sigma_{mU}) &= 1 - \exp(-\sigma_{mU}/\sigma_{m0})^{\beta_m} \end{aligned} \tag{39}$$

The scale and shape parameters are related to the mean and standard deviation values of the strength through the well-known formulas. For example, for interfacial strength these formulas are

$$\langle \tau_d \rangle = \tau_0\Gamma(1 + 1/\beta_d); \qquad D_{\tau_d} = \langle \tau_d \rangle \sqrt{\frac{\Gamma(1 + 2/\beta_d)}{\Gamma^2(1 + 1/\beta_d)} - 1} \tag{40}$$

Let us consider graphite/epoxy composites. The experimental elastic and strength properties of the constituents are presented in Table 1.

The following parameters have been adopted for the numerical strengths calculation of carbon/epoxy composite. Elastic constants and mean strengths of the constituents are taken from Table 1. In Refs. 26 and 27 there are no experimental data for the constituents strength's scatter. According to Ref. 28, for carbon fibers β_f varies from three to six. According to the experimental study[29] of the ultimate strengths of the fiber/matrix interfacial bond of some fiber/matrix combinations the scatter in ultimate interfacial strengths is 8–18% [interfacial shear stress (ISS) range for carbon fiber/polycarbonate matrix is 62.2–90.6 MPa and 67.7–97.0 MPa for carbon fiber/polysulfone matrix. Using the formulas for the standard deviation (40) one can obtain the following range for the parameter of the interfacial strength scatter: $\beta_d \approx 6$–12. A similar range for β_d variation has been obtained in Ref. 25: for Modmor-1/epoxy specimen $\beta_d = 5.4$ (coefficient of variation 0.21) and for T-300B/PA-6 $\beta_d = 10.8$ (coefficient of variation 0.11). Based on these experimental data β_f and β_d are chosen as $\beta_f = 6$ and $\beta_d = 6$. The rest of the parameters have been adopted as $\beta_m = 6$; $\tau_R = \kappa\langle \tau_d \rangle$, where κ varies as $0.05 \le \kappa \le 0.1$; composite volume $V_0 = 10^3$ mm; and $d_f = 10\ \mu$m.

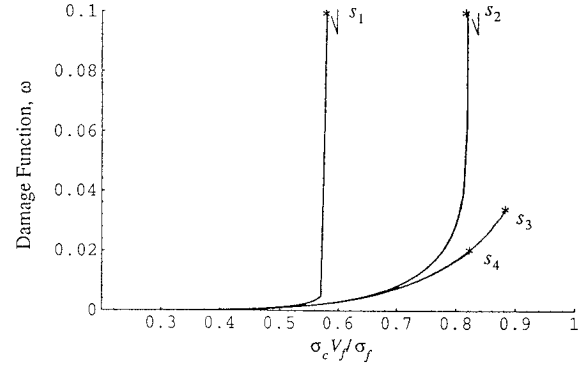

Fig. 4 Damage function ω for composites with various interfacial shear strength, $\langle \tau_d \rangle$ = 10 MPa (s_1), -70 MPa (s_2), -160 MPa (s_3), and -200 MPa (s_4).

Results and Discussion

ODEPACK solver[30] is utilized for numerical simulation of the system (20). The computer code is written in Fortran.

Figure 4 shows damage accumulation with the loading. Four cases of interfacial shear strength are shown. At low interfacial strength (curves s_1 and s_2), damage grows at an unstable rate when a certain loading level is reached. Stable damage growth occurs for composites with high interfacial shear strength (curves s_3 and s_4). The probability that a fiber break will be accompanied by a long interface debonding is high in composites with a relatively low interfacial shear strength. The stress concentration in neighboring intact fibers is negligible in such composites. The damage accumulation is primarily due to random fiber breaks. The unstable growth of fiber breaks occurs when intact fibers are unable to withstand the increasing share of the longitudinal stress [$\sigma^* = \sigma/(1 - \omega)$]. When the interfacial shear strength is high enough to prevent interface debonding, the final failure is governed by the unstable growth of a single fracture much before the damage in the composite reaches a significant level.

Results shown in Fig. 5 corroborate the arguments presented in the last paragraph. The probabilities of having damage states with various fiber breaks as a function of applied stress are shown in this figure. The curves represent probabilities of developing at least one damaged state containing no less than i adjacent broken fibers. Figure 5a represents a low interfacial strength. At a low bonding strength, the separate curves for each i value signifies that fracture states with a low number of fiber breaks continue to grow, and the probability of appearance of a single macrocrack stays low up to the final failure. The final failure occurs suddenly due to the coalescence of a large number of damage states with a low number of multiple fiber breaks. Figure 5b represents a high interfacial strength. In this case, the probability of growth of a damage state with a large number of adjacent fiber breaks approaches a limiting value and, therefore, the final failure is a result of single macrocrack formation. At the time of the final failure occurring in this manner,

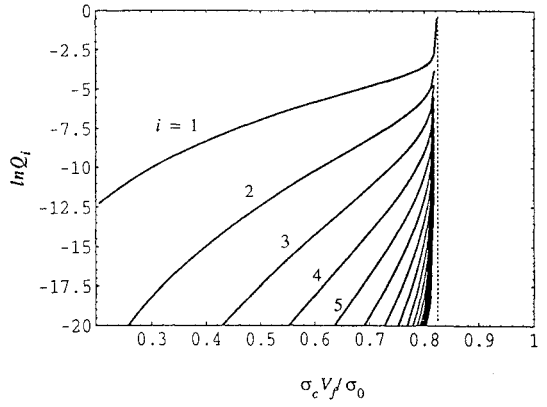

a)

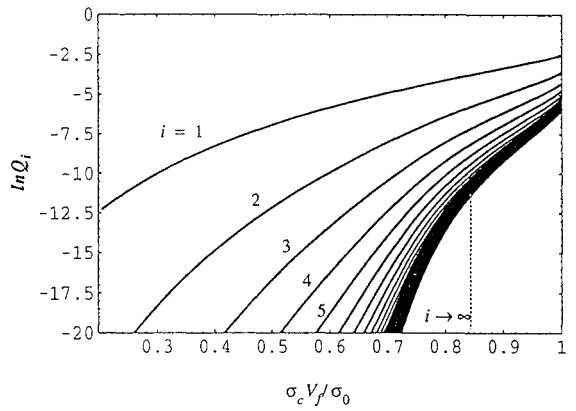

b)

Fig. 5 Probabilities of multiple fiber breakdowns for the composite with low and high, fiber/matrix interfacial strength; $\tau_R/\langle\tau_d\rangle$ = 0.05: a) low strength $\langle\tau_d\rangle$ = 70 MPa, and b) high strength $\langle\tau_d\rangle$ = 200 MPa.

the amount of damage stays relatively low as shown by the asterisks on curves s_3 and s_4 in Fig. 4. For fracture mode due to a single macrocrack development the damage level just before the final failure is about 2~4% which is in a good agreement with previous simulations and experimental results for highly oriented nylon as well as for carbon/epoxy and boron/epoxy composites.[7,31,32]

The influence of the interfacial shear strength on the composite strength is shown in Fig. 6. Two parametric levels of frictional stress at the debonded interface are presented by two curves in the figure. Experimental values of the strength taken from Ref. 27 are presented by vertical bars in the same figure. The s_1, s_2, s_3, and s_4 points correspond to the curves in Fig. 4. There are two distinct portions of the plots of composite strength as a function of the interfacial shear strength. At relatively high interfacial shear strength, high stress concentration level introduces a high probability of macrocrack development. This fracture mode leads to reduction in the composite strength with the increased interfacial strength. Nevertheless, after a certain value of the interfacial shear strength debonding does not occur, and a further increase in the interfacial shear strength has no influence on the composite strength.

At relatively low interfacial strength, the relationship between the interfacial shear strength and the composite strength is governed by the coalescence of the arrested or slowly developing damage states. At lower values within this range of the interfacial shear strengths, large debonding lengths increase the damage level and, consequently, the possibility of percolation at lower stress levels. At higher values within this range, the composite strength improves because debonding length decreases and the percolation occurs at higher stress levels.

The results suggest that there is an optimum value for the interfacial shear strength that gives the maximum composite strength. This kind of influence of the interfacial shear strength on the carbon/aluminium composite strength has been experimentally observed in Ref. 33.

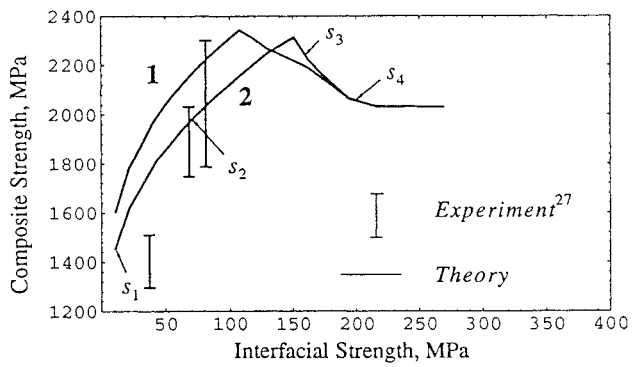

Fig. 6 Graphite/epoxy composite strength variation with fiber/matrix interfacial shear strength; $\tau_R/\langle\tau_d\rangle$ = 0.10 (1) and τ_R/τ_d = 0.05 (2).

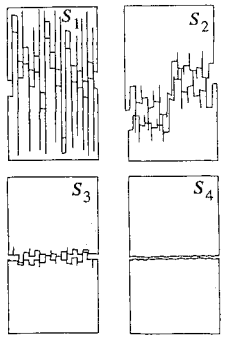

Fig. 7 Schematic representation of fracture surfaces.

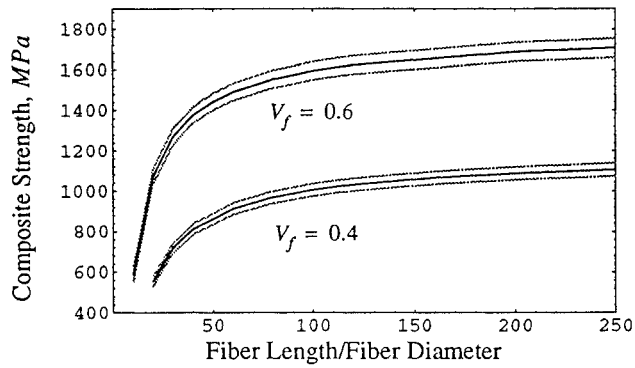

Fig. 8 Carbon/epoxy composite strength variation with fiber length $\langle\tau_d\rangle/\langle\sigma_{mU}\rangle$ = 0.5; solid lines, composite mean strength and dashed lines, composite strengths standard deviation.

The magnitude of the interfacial strength and its influence on the relative amounts of interface failure determine the overall appearance of the fracture surface. This is illustrated in Fig. 7. For a weak interface bonding the composite exhibits extensive debonding, and the fracture surface has a very rough appearance with large amounts of fibers pulled out (s_1, s_2). For a strongly bonded fiber/matrix interface there is only a small amount of debonding and the fracture surface is rather smooth (s_3, s_4).

The preceding results are for continuous fiber reinforced composites. The following results are for short fiber composites. The effect of the fiber length on the composite strength is shown in Fig. 8. The shorter is the fiber length, the higher is the probability that a unit cell contains a short fiber end. Also, the probability of encountering a fiber end during crack propagation is higher. The composite strength decreases with the decreasing length of short fibers due to these reasons. But this relationship is not linear because the probability of finding a fiber end is inversely proportional to the short fiber length [see Eq. (15)]. It follows from Eqs. (2) and (15) that the higher is the fiber volume fraction, the lower is the probability of finding a fiber end inside a unit cell and, consequently, the composite strength is higher. This effect is presented in Fig. 9.

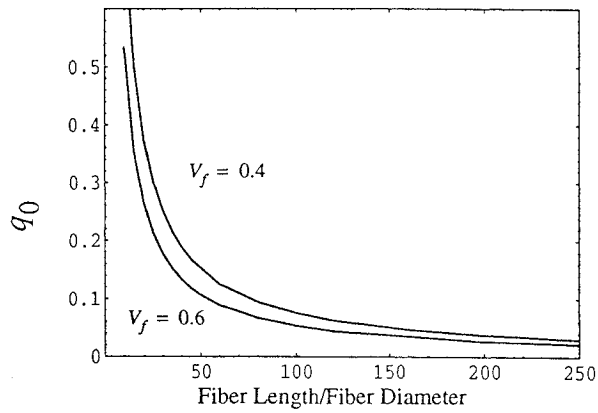

Fig. 9 Probability q_0 of finding a short fiber end inside a unit cell.

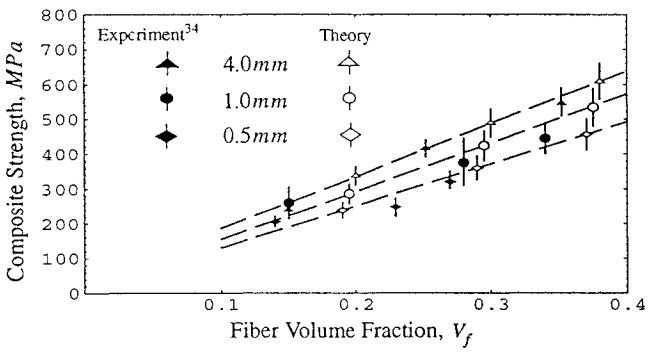

Fig. 10 Composite mean strength and its variance for aligned AS2 carbon fiber composites.

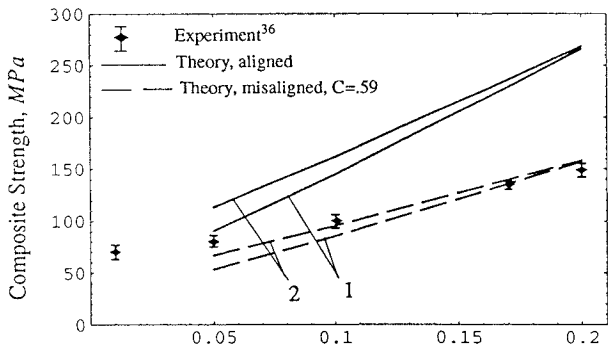

Fig. 11 Strength variation with fiber volume fraction for glass fibers in polyamide 6.6 matrix, average fiber length $\bar{l}$ = 0.5 mm; $\langle\sigma_{mU}\rangle/\langle\tau_d\rangle$ = 0.61 (1), and $\langle\sigma_{mU}\rangle/\tau_d$ = 0.92 (2).

Composite strength variations calculated by formulas (33–35) are also presented in Fig. 8 by dashed lines. Mainly, this variance is the result of scatter in the fiber strength properties.

The strength simulation results for short-fiber reinforced thermosets are presented in Fig. 10. The composite is Hercules AS2 carbon fibers in Shell EPON 828 resin. The input data for the calculations are from Ref. 35: $E_f = 234$ GPa, $E_m = 3.6$ MPa, fiber strength $\langle\sigma_f\rangle = 2.8 \pm 0.5$ GPa, matrix strength $\langle\sigma_{mU}\rangle \approx 30$ MPa, and fiber diameter $d_f = 0.08$ mm. There are no data given about fiber/matrix bond strength in Ref. 34, and so the assumption $\langle\tau_d\rangle \gg \langle\sigma_{mu}\rangle$ has been adopted for the calculation. The scatter in fiber strength is about 20% which corresponds to $\beta_f \approx 6$. The rest of the parameters are chosen as $\beta_m = 6$ and $V_0 = 10^3$ mm. As it can be seen from Fig. 10, the correlation between experimental data and theoretical strengths prediction is rather close.

The relation between a short fiber composite strength, E-glass/PA66, and the volume fraction of fibers is shown in Fig. 11. Typical data for polyamide thermoplastic reinforced with glass fibers have been used from Ref. 36. Mechanical properties for E-glass (Vetrotex) are $E_f = 73$ GPa and $\langle\sigma_f\rangle = 3.4$ GPa. Mechanical properties of thermoplastic resin (polyamide) are $E_m = 2.0$ GPa, $\langle\sigma_{mU}\rangle = 70 \div 84$ MPa, and $\langle\tau_d\rangle = 65$ MPa (Ref. 36). Fiber diameter $d_f = 0.01$ mm and specimen volume $V_0 = 400$ mm. The solid lines in Fig. 11 correspond to the aligned short-fiber composite for two different matrix strengths (curves 1 and 2). The experimental results presented in Ref. 36 are for the composite with imperfectly aligned fibers. It has been reported there that the orientation constant C varies in a range $0.5 \le C \le 0.6$ as the fiber volume fraction changes from $V_f = 0.05$ to $V_f = 0.2$. The results of the strength recalculation by making use of Eq. (3) with $C = 0.59$ are shown in Fig. 11 by the dashed lines. The agreement between the experimental results and the theoretical prediction is satisfactory.

Conclusion

A theoretical model for describing fracture process, starting from random fracture nucleations to the final failure, in unidirectional continuous and short-fiber reinforced composites is presented. The model incorporates the primary and secondary fracture mechanisms and their interaction in a cohesive manner. The numerical simulation suggests that there is an optimum value for the interfacial shear strength that gives the maximum composite strength. The magnitude of the interfacial shear strength also determines the overall appearance of the fracture surface. The composite strength increases with increasing length of short fibers. However, the effect is insignificant for long fibers. In addition to these predictions, the simulation results are compared with some of the available experimental observations and are found to be in reasonably good agreement. The authors are continuing the research to incorporate other loading conditions. Further research in this direction may significantly improve our ability to understand the structural behavior of materials up to the final failure. The understanding of various parameters that affect the useful life of structures will also help us design better composites.

References

[1]Rosen, B. W., "Tensile Failure of Fibrous Composites," *AIAA Journal*, Vol. 2, No. 11, 1964, pp. 1985–1991.

[2]Zweben, C., "Tensile Failure of Fiber Composites," *AIAA Journal*, Vol. 6, No. 12, 1968, pp. 2325–2332.

[3]Harlow, D. G., and Phoenix, S. L., "The Chain-of-Bundles Probability Model for the Strength of Fibrous Materials I: Analysis and Conjectures," *Journal of Composite Materials*, Vol. 12, April 1978, pp. 195–214.

[4]Harlow, D. G., and Phoenix, S. L., "The Chain-of-Bundles Probability Model for the Strength of Fibrous Materials II: A Numerical Study of Convergence," *Journal of Composite Materials*, Vol. 12, July 1978, pp. 314–334.

[5]Fukuda, H., and Kawabata, K., "Strength Estimation of Unidirectional Composites," *Transactions of the Japan Society of Composite Materials*, Vol. 2, 1976, pp. 59–62.

[6]Batdorf, S. B., "Tensile Strength of Unidirectionally Reinforced Composites-I," *Journal of Reinforced Plastics and Composites*, Vol. 1, 1982, pp. 153–164.

[7]Tamuzs, V. P., "Some Peculiarities of Fracture in Heterogeneous Materials," *Fracture of Composite Materials*, edited by G. C. Sih and V. P. Tamuzs, Martinus Hijhoff, Boston, MA, 1982, pp. 131–137.

[8]Ovchinskii, A. S., *Fracture Processes in Composite Materials: Computer Imitation of Micro- and Macro- Mechanisms* (in Russian), Nauka, Moscow, 1988, Chaps. 2, 3.

[9]Fukuda, H., and Chou, T.-W., "A Probabilistic Theory for the Strength of Short Fibre Composites," *Journal of Material Science*, Vol. 16, No. 4, 1981, pp. 1088–1096.

[10]Chou, T.-W., and Hikami, F., "A Probabilistic Theory of the Strength of Short-Fiber Composites," *Advances in Aerospace Structures, Materials and Dynamics: The Winter Annual Meeting ASME* (Boston, MA), American Society of Mechanical Engineers, New York, Nov. 1983, pp. 97–101.

[11]Friedman, E., "A Tensile Failure Mechanism for Whisker Reinforced Composites," 22nd Annual Meeting of the Reinforced Plastics Division of the SPI, Washington, DC, Feb. 1967.

[12]Wetherhold, R. C., "Probabilistic Aspects of Strength of Short-Fibre Composite with Planar Fibre Distribution," *Journal of Material Science*, Vol. 22, No. 2, 1987, pp. 663–669.

[13]Hillig, W. B., "Effect of Fibre Misalignment on Fracture Behavior of Fibre-Reinforced Composites. Part II. Theoretical Modelling," *Journal of Material Science*, Vol. 29, No. 4, 1994, pp. 899–920.

[14]Mendelson, A., "Plastic Stress-Strain Relations," *Plasticity: Theory and Applications*, Krieger, Malabar, FL, 1983, pp. 98–134.

[15]Hedgepeth, J. M., "Stress Concentrations in Filamentary Structures," NASA TN D-882, May 1961.

[16]Hedgepeth, J. M., and Van Dyke, P., "Local Stress Concentration in Imperfect Filamentary Composite Materials," *Journal of Composite Materials*, Vol. 1, July 1967, pp. 294–309.

[17]Budiansky, B., and Hutchinson, J. W., "Matrix Fracture in Fiber-Reinforced Ceramics," *J. Mech. Phys. Solids*, Vol. 34, No. 2, 1986, pp. 167–189.

[18]Tsai, W. B., and Mura, T., "Micromechanics of Matrix Cracking in Fiber-Reinforced Brittle-Matrix Composites," *Composites Engineering*, Vol. 3, No. 10, pp. 929–944.

[19]Li, S. H., Shah, S. P., Li, Z., and Mura, T., "Micromechanical Analysis of Multiple Fracture and Evaluation of Debonding Behavior for Fiber-Reinforced Composites," *International Journal of Solids Structures*, 1993, Vol. 30, No. 11, pp. 1429–1459.

[20]Nguyen, T.-H. B., and Yang, J.-M., "Elastic Bridging for Modeling Fatigue Crack Propagation in a Fiber-Reinforced Titanium Matrix Composite," *Fatigue and Fracture of Engineering Materials and Structures*, Vol. 17, No. 2, 1994, pp. 119–131.

[21]Broutman, L. J., "Measurement of the Fiber Polymer Matrix Interfacial Strength," *Interfaces in Composites*, York, PA, 1969, pp. 27–41.

[22]Hull, D., "Fibre Pull-Out," *An Introduction to Composite Materials*, Cambridge Univ. Press, Cambridge, New York, 1981, pp. 142–145.

[23]Gillespie, D. T., "Jump Markov Processes with Discrete States," *Markov Processes*, Academic, Boston, MA, 1992, pp. 317–373.

[24]Dzenis, Y. A., and Joshi, S. P., "Inhomogeneous Anisotropic Percolation: 2D Numerical Threshold Analysis," *Physical Review B*, No. 5, Feb. 1994.

[25]Andersons, J., and Tamuzs, V., "Fiber and Interface Strength Distribution Studies With the Single-Fiber Composite Test," *Composites Science and Technology*, Vol. 48, 1993, pp. 57–63.

[26]Madhukar, M. S., and Drzal, L. T., "Fiber/Matrix Adhesion and Its Effect on Composite Mechanical Properties: I. Inplane and Interlaminar Shear Behavior of Graphite/Epoxy Composites," *Journal of Composite Materials*, Vol. 25, No. 8, 1991, pp. 932–957.

[27]Madhukar, M. S., and Drzal, L. T., "Fiber/Matrix Adhesion and Its Effect on Composite Mechanical Properties: II. Longitudinal (0°) and Transverse (90°) Tensile and Flexure Behavior of Graphite/Epoxy Composites," *Journal of Composites Materials*, Vol. 25, No. 8, 1991, pp. 958–991.

[28]Tamuzs, V. P., Azarova, M. T., Bondarenko, B. M., Gutans, Y. A., Korabelnikov, J. G., Pikshe, P. E., and Siluyanov, O. G., "Fracture of Unidirectional Carbon Fibre Plastics and Realization of Fibre Strength Properties in Them," *Mechanics of Composite Materials*, Vol. 18, 1982, pp. 34–41 (in Russian).

[29]Latour, R. A., and Black, J., "Fiber/Matrix Interfacial Bond Ultimate and Fatigue Strength Characterization in a 37°C Dry Environment," *Journal of Composite Materials*, Vol. 26, No. 2, 1992, pp. 256–273.

[30]Hindmarsh, A. S., "ODEPACK, A Systematized Collection of ODE Solvers," *Scientific Computing*, edited by R. S. Stepleman et al., Vol. 1 IMACS Transactions on Scientific Computation, North-Holland, Amsterdam, 1983, pp. 55–64.

[31]Tikhomirov, P. V., and Yushanov, S. P., "Volumetric Fracture Mechanism of Materials Having a Heterogeneous Structure," *Polymer Mechanics* (Riga), No. 3, 1978, pp. 462–469.

[32]Kuksenko, V. S., and Tamuzs, V. P., "Localization of the Fracture Processes," *Fracture Micromechanics of Polymer Materials*, Martinus Nijhoff, Boston, MA, 1981, pp. 139–166.

[33]Salibekov, S. Y., Zabolotsky, A. A., Kontsevich, I. A., and Fadyukov, Y. M., "Factors Having Influence on Structure and Properties Formation in Al–Carbon Composite Materials," *Poroshkovaya Metallurgiya* (*Powder Metallurgy*), No. 2, 1977, pp. 58–64 (in Russian).

[34]Piggott, M. R., Ko, M., and Chuang, H. Y., "Aligned Short-Fibre Reinforced Thermosets: Experiments and Analysis Lend Little Support For Established Theory," *Composites Science and Technology*, Vol. 48, 1993, pp. 291–299.

[35]Hancox, N. L., and Mayer, R. M., "Properties," *Design Data For Reinforced Plastics*, Chapman and Hall, London, 1994, pp. 39–49.

[36]Curtis, P. T., Bader, M. G., and Bailey, J. E., "The Stiffness and Strength of a Polyamide Thermoplastics Reinforced With Glass and Carbon Fibres," *Journal of Materials Science*, Vol. 13, No. 2, pp. 377–390.